Published in final edited form as:
Microsurgery. 2012 October ; 32(7): 552–562. doi:10.1002/micr.22036.

Axonal Regeneration and Motor Neuron Survival after Microsurgical Nerve Reconstruction

Ida K. Fox, M.D.[1,2], **Michael J. Brenner, M.D.**[3,4], **Philip J. Johnson, Ph.D.**[1,2], **Daniel A. Hunter, R.A.**[1,2], and **Susan E. Mackinnon, M.D.**[1,2,*]

[1]Division of Plastic and Reconstructive Surgery, Washington University School of Medicine, Saint Louis, MO

[2]Department of Surgery, Washington University School of Medicine, Saint Louis, MO

[3]Division of Otolaryngology–Head and Neck Surgery, Southern Illinois University School of Medicine, Springfield, IL

[4]Department of Surgery, Southern Illinois University School of Medicine, Springfield, IL

Abstract

Rodent models are used extensively for studying nerve regeneration, but little is known about how sprouting and pruning influence peripheral nerve fiber counts and motor neuron pools. The purpose of this study was to identify fluctuations in nerve regeneration and neuronal survival over time. One hundred and forty-four Lewis rats were randomized to end-to-end repair or nerve grafting (1.5 cm graft) after sciatic nerve transection. Quantitative histomorphometry and retrograde labeling of motor neurons were performed at 1, 3, 6, 9, 12, and 24 months and supplemented by electron microscopy. Fiber counts and motor neuron counts increased between 1 and 3 months, followed by plateau. End-to-end repair resulted in persistently higher fiber counts compared to the grafting for all time points ($P < 0.05$). Percent neural tissue and myelin width increased with time while fibrin debris dissipated. In conclusion, these data detail the natural history of regeneration and demonstrate that overall fiber counts may remain stable despite pruning.

Nerve transection involves severing of defined pathways, such that old pathways must be repaired and new pathways created.[1] The disruption of these pathways not only introduces the potential for errors in axonal guidance but also the possibility of loss of regenerating fibers at the interface of proximal and distal stumps. These conditions differ physiologically and functionally from crush injury, in which axonal regeneration can usually proceeds through preserved pathways. From a practical standpoint, if a crushed nerve is decompressed promptly—and the obstacles to healing thus removed—the prognosis is favorable. In contrast, nerve transection poses challenges from the standpoints of both reinnervation and functional recovery, particularly if nerve grafting is needed to bridge a

*Correspondence to: Susan E. Mackinnon, MD, Shoenberg Professor and Chief, Division of Plastic and Reconstructive Surgery, Washington University School of Medicine, Box 8328, 660 South Euclid Avenue, Saint Louis, MO 63110. mackinnons@wudosis.wustl.edu.

nerve gap. Experimental approaches to enhance recovery have focused on transection and nerve gap injuries, variously investigating pharmacologic agents,[2] neurotrophic factors,[3] novel scaffolds, and conduits,[4] blockade of factors that inhibit regeneration,[5] cellular transplantation,[6,7] and electrical stimulation.[8–12]

The number of regenerating nerve fibers present and the number of surviving motor neuron may fluctuate over time, a tendency that may confound experimental studies of nerve regeneration.[13] When axons are severed, a complex sequence of events begins that variously involves degeneration, sprouting, elongation, and pruning of nerve fibers. The number of fibers present is affected by how many motor neurons cell bodies remain viable, the number of axon sprouts emerging from each cut nerve fiber, the number of fibers misrouted in a retrograde direction, and the fibers that are trapped in neuromata or pruned.

In most experimental studies, the novel treatment is pitted against the gold standards of end-to-end nerve repair or interposition nerve grafting at a fixed time point after injury. Such studies are predicated upon the assumption that the time point is selected will allow for meaningful comparison. But, in some cases, only a finite window exists for making valid comparisons between groups.[14] In this study, we investigated the natural course of nerve regeneration and motor neuron survival after sciatic nerve end-to-end repair and interposition nerve grafting. Animals were evaluated at time points spread over 2 years to establish longitudinal patterns for regeneration and motor neuron survival. It was hypothesized that nerve fiber counts would spike initially, related to sprouting, and then stabilize whereas the number of motor neuron cell bodies in the spinal cord ventral horn was predicted to remain stable.

Materials and Methods

Animal Provisions

A total of 180 male Lewis rats (60-day-old, 250 g, Charles River Laboratories, Wilmington, MA) were involved in this study, including 144 rats enrolled in experiment groups and 36 additional animals that served as bilateral sciatic nerve donors. All feeding and weaning procedures were performed under direction of Division of Comparative Medicine staff. Animals were housed in a central animal care facility and provided a balanced rodent diet with water ad libitum. Following surgical procedures, animals were recovered in a warm environment under direct supervision and then promptly returned to the central animal facility. Animals were monitored daily for signs of wound infection, weight loss, impaired grooming, or other evidence of morbidity. All experimental procedures and interventions as well as housing, diet, and animal care regimens were performed in strict accordance with guidelines from the National Institutes of Health. The experimental protocol was approved by the Institutional Animal Studies Committee.

Experimental Design

Animals were randomly assigned to undergo either nerve transection with end-to-end repair or nerve grafting of a 5 mm nerve gap with 1.5 cm interpositional nerve grafting. The 144 experimental animals were equally divided between the two groups. Animals were then

randomly designated for assessment at 1, 3, 6, 9, 12, or 24 months endpoints, for 12 groups, with an average of 12 experimental animals per group. Tissue analysis of the harvested sciatic nerves involved use of quantitative histomorphometry for assessment of nerve regeneration distal to the end-to-end repair or distal to the isograft. In addition, labeling of the motor neuron cell bodies of the ventral horn was performed to assess motor neuron survival in four rats from each group. For labeled animals, the spinal cord ventral horn was harvested and the labeled cell bodies were counted. Electron microscopy was performed on specimens at the 1 month endpoint to evaluate for the presence of immature, unmyelinated fibers not detectable with light microscopy.

Nerve Dissection, Neurorrhaphy, and Nerve Grafting

Anesthesia was induced with an intramuscular injection of ketamine (Fort Dodge Animal Health, Fort Dodge, IA) at a dose of 50 mg/kg and medetomidine HCl (Pfizer Animal Health, Exton, PA) at a dose of 0.2 mg/kg. All surgical procedures were performed aseptically under 16X magnification with a Wild M651 operating microscope (Leica Microsystems, Deerfield, IL). For all animals, the sciatic nerves were identified with sharp muscle-splitting incisions followed by blunt dissection. For experimental animals undergoing nerve transection and end-to-end repair, the sciatic nerve was divided 0.5 cm proximal to the sciatic trifurcation and then neurorrhaphy performed with 6 interrupted epineurial sutures placed under microscope with 9–0 nylon suture. Muscle and skin were then closed with absorbable suture.

For animals undergoing nerve grafting, sciatic nerves were harvested from isologous donor animals immediately prior to the grafting procedure. For donor nerve harvest, sciatic nerves were identified bilaterally and a 1.5 cm segment of the sciatic nerve was isolated and harvested as the nerve graft (experimental animals underwent unilateral nerve surgery, so each donor animal provided sciatic nerve tissue for two experimental animals). The right sciatic nerve was then identified in the recipient animal, transected proximal to the sciatic nerve trifurcation, and 5 mm of nerve resected. This 5 mm defect allowed for ease of graft interposition, given retraction of the cut nerve ends that occurs after division of the nerve. The 1.5 cm donor nerve graft was inset in reverse orientation, interposed, and coapted with 6 interrupted 9–0 nylon microepineurial sutures.

Harvest of Sciatic Nerve and Spinal Cord Motor Neurons

Harvest was performed at 1, 3, 6, 9, 12, or 24 months from the original surgery. Animals were reanesthetized and nerves exposed as in the original surgical procedure. Sciatic nerves to be used for histomorphometry were harvested *en block*, taking care to obtain at least 5 mm of tissue distal to the suture line or graft in all cases. The distal nerve was identified, dissected clear of surrounding tissues, and placed in fixative. Animals were then euthanized by intracardiac pentobarbital injection (Delmarva Laboratories, Midlothian, VA) and spinal tissue collected for motor neuronal analysis. The spinal cords were harvested for motor neuron cell count analysis from those animals in each group that had undergone retrograde tracer injection. The spinal cord harvest was performed from posterior approach with dissection of erector spinae musculature followed by laminectomy and atraumatic removal and fixation of the spinal cords.

Retrograde Labeling and Fluorescence Microscopy

Quantitative fluorescence microscopy was performed to assess origin of axons within the spinal cord using methods previously described.[15] At 72 hours prior to harvest, 2 ml of 2% Fast-blue retrograde tracer (Sigma, St. Louis, MO) was injected with a Hamilton syringe into the nerve 5 mm distal to the repair site. Harvested spinal cords were stored in 4% paraformaldehyde overnight and subsequently cut into 40-micron longitudinal frozen sections on a cryostat. Specimens were then viewed by fluorescence microscopy with an A2 filter to determine total number of labeled motor neuron cell bodies in the ventral horn. The number of fluorescently labeled motor neurons was quantified in each serial section. Counting was performed within 2 hours after tissue sectioning to avoid possible bias from spread of label to surrounding cells and to prevent loss of signal. A low light CCD camera was used to visualize the brilliantly labeled fluorescent blue motor neurons. An image board was then used to capture images, and cell bodies were counted by image analysis using the program PAX-IT™ (Leco Corporation St Joseph, MI). An observer blinded to the experimental groups performed all measurements.

Histomorphometric Evaluation and Electron Microscopy

Sciatic nerve specimens were fixed in a cold, buffered 3% glutaraldehyde solution for 24 hours, post-fixed with osmium tetroxide, and embedded in Araldite 502 (Polysciences, Warrington, PA). Next, 1 μm-thick cross-sections were cut with an LKB III Ultramicrotome (LKB-Produkter A.B., Bromma, Sweden) and stained with 1% toluidine blue. Under light microscopy, these stained cross-sections were evaluated for overall nerve architecture, quality and quantity of regenerated nerve fibers, extent of myelination, and presence of Wallerian degeneration (WD).

Using an automated digital image-analysis system linked to morphometry software (Leco Instruments, St. Joseph, Michigan), the microscope image was digitized and displayed on a video monitor with a calibration of 0.125 μm/pixel. Computer analysis of the digitized information based on gray and white scales allowed measurements of total fascicular area and total fiber number in the recipient nerve 5 mm distal to the graft repair as well within the midgraft. At 1000X magnification, 6 randomly selected fields per nerve, or a minimum of 500 myelinated fibers, were evaluated for myelin width, axon width, and fiber width. From these, calculations of nerve fiber density (fibers/mm^2), total number of myelinated fibers, myelin width, percentage of neural tissue (100X neural area/intrafascicular area), and fibrin debris were made. An observer blinded to the experimental groups performed all measurements.[16]

Electron microscopy was performed on specimens obtained from 1 month harvest to evaluate for presence of unmyelinated fibers, as well as for qualitative analysis including assessment of WD, Schwann cell proliferation, and any early restoration of neural architecture. Ultrathin sections were cut with an LKB III ultramicrotome (LKB Productur, A.B. Bromma, Sweden), stained with uranyl acetate–lead acetate and examined on a Zeiss 902 electron microscope (Zeiss Instruments, Chicago IL).

Statistical Analysis

Statistica (StatSoft, Tulsa, OK) was used to analyze statistical data. A one-way analysis of variance (ANOVA) was performed for comparisons across the serial time points for both end-to-end repair and nerve grafting groups. Statistical procedures were based on the distribution frequency of all of the data. If the analysis demonstrated significance, then the means of variables from specific groups were compared using the Student-Newman-Keuls test. Sample size analysis was based on prior laboratory data on nerve regeneration involving comparison between groups for motor neuron cell body counts and histomorphometry fiber count parameters. In all cases, statistical significance was set at $P < 0.05$.

Results

General Considerations

The surgical procedures were well tolerated in all animals, although attrition of animals related to advanced age was observed in the animals randomized to the 24 month group (of that cohort of 24 animals, 16 animals survived to completion of the study and 8 died; no necropsy was performed in the old animals that died). Otherwise, animals demonstrated normal activity and feeding patterns without weight loss, wound infection, or evidence of systemic illness.

Qualitative Analysis

Representative photomicrographs of nerves harvested at serial time points after end-to-end repair and nerve grafting are shown in Figures 1 and 2, respectively. While the number of regenerating nerve fibers remained relatively stable after 3 months, nerve fibers assumed a more mature appearance over the course of subsequent assessments. At 12 and 24 months, nerves appeared more heavily myelinated, had a greater quantity of neural tissue present, and had demonstrated less neural debris than at 3 months. The number of fibers was persistently greater after cut and repair than after nerve grafting, indicative of a decrement in regeneration from either crossing a second suture line or an increased regeneration distance. The observation of a leveling off fiber counts at 3 months was mirrored by a similar plateau in counts of motor neurons labeled by retrograde tracing at 3 months. Histological sections from the retrograde labeled spinal cord ventral horn are shown in Figure 3.

Histomorphometric Evaluation

The pattern of nerve regeneration after injury followed parallel, but nonintersecting, courses for the cut and repair versus nerve grafting groups (Fig. 4). The normal uninjured rat sciatic nerve contains ∼8,000 myelinated nerve fibers. In the cut and repair group, fiber counts were approaching maximal levels by the initial 1 month endpoint (mean fiber counts were 9,102 ± 3,530 at 1 month versus 13,850 ± 3,897 at 3 months). In contrast, amongst the grafted animals, no myelinated nerve fibers had crossed the second suture distal to the nerve isograft (mean fiber count undetectable at 1 month versus 8,688 ± 1,623 at 3 months). Both groups had reached a plateau by 3 months, but the absolute value at which fiber counts leveled off were significantly different at all time points ($P < 0.05$). The mean fiber counts

in the cut and repair group during months 3, 6, 9, 12, and 24 months ranged from 12,219 ± 2,423 to 13,850 ± 3,897 whereas the mean fiber counts in the nerve isograft group during the same period ranged from 8,205 ± 1,533 to 9,366 ± 2,571. The findings for nerve density (fibers per mm^2) were similar, with both groups demonstrating a plateau at 3 months (24,573 ± 3,857 for cut and repair versus 21,972 ± 4,023 for nerve graft). Difference in nerve density was not significantly different between the groups.

The tendency for early plateau was less evident for other histomorphometric parameters. Percent neural tissue and myelination progressed gradually over the 24 month period observed. For the cut and repair group, the percent nerve increased from 18.15 ± 9.06 at 1 month to 36.71 ± 7.74 at 3 month to and eventual peak at 52.47 ± 9.72 at 24 months. For the nerve graft group, percent myelinated nerve distal to the graft increased from undetectable at 1 month to 26.56 ± 5.59 at 3 months to a peak of 45.90 ± 7.49 at 12 months. Myelinated fiber width exhibited a similar pattern. In the cut and repair group, myelinated fiber width (measured in micrometers) gradually increased from 3.31 ± 0.25 at 1 month to 3.55 ± 0.16 at 3 months to peak at 4.30 ± 0.18 at 12 months. In the nerve graft group, myelinated fiber width distal to the nerve graft increased from undetectable at 1 month to 3.23 ± 0.17 at 3 months to peak at 4.24 ± 0.09 at 12 months. Most of the clearance of fiber debris occurred over the course of the first 9 months for both experimental groups. Notably, the peak for fiber debris was significantly higher in the isograft group (21.16 ± 4.23) than in the end-to-end repair group (5.71 ± 2.82).

Histomorphometric analysis of sections taken from the mid-portion of isografts showed patterns of regeneration consistent with those observed in the sections distal to the nerve graft. Total fiber counts from these midgraft sections increased from 1,508 ± 772 at 1 month to 15,437 ± 4,669 at 3 months with peak at 6 months of 17,941 ± 2,777, after which these values had a plateau. Similarly, nerve density (fibers per mm^2) detected in midgrafts increased rapidly from 1,417 ± 681 at 1 month to a peak of 31,428 ± 9,008 at 3 months followed by plateau through 24 months. The percent nerve steadily increased through the first year, with percent values of 1.26 ± 0.66 at 1 month, 34.79 ± 0.18 at 3 months, 39.99 ± 5.26, 51.96 ± 4.86 at 12 months, and 50.44 ± 7.6 at 24 months. The mean fiber width was 2.85 ± 0.20 at 1 month and gradually increased to a peak of 2.79 ± 0.26 at 24 months. The percent fibrin debris present in nerve sections showed a similar time course of decline as the debris was cleared, but a longer tail was apparent. Fibrin debris constituted 23.24 ± 4.2% of nerve area at 1 month, 7.54 ± 6.11% of area at 3 months, and gradually tapered down to a nadir of 0.26 ± 0.47% of area at 24 months. No statistical difference was observed in these histomorphometric parameters ($P > 0.05$).

Motor Neuron Pool Assessment

The motor neuron pool assessment, which was determined by retrograde labeling of cell bodies in the spinal cord ventral horn, showed evidence of motor neuron regeneration at 1 month in both groups. Mean cell body counts at 1 month were 1,168 ± 195 for the cut and repair group and 394 ± 187 for the nerve isograft group. No statistically significant changes were present after 3 months. At 3 months, mean motor neuron counts were 1,046 ± 279 for cut and repair versus 760 ± 221 for the nerve isograft group, mirroring the findings on

morphometry of decreased absolute motor neuron regeneration distal to a nerve graft compared to a single suture line. Due to interanimal variability, this difference was not significant. The presence of labeled motor neuron cell bodies at 1 month in the grafted group suggested that immature, unmyelinated fibers (undetectable with light microscopy) might have allowed for this uptake of retrograde label.

Electron Microscopy

Evaluation with electron microscopy confirmed the presence of regenerating fibers in both experimental groups at 1 month. Whereas both myelinated and unmyelinated fibers were present in the transection and repair group, only unmyelinated fibers were present in the nerve graft group. Both groups had evidence of ongoing WD, but these findings were more prominent in the nerve graft group. In both groups, numerous Schwann cells were observed in close association with immature fibers, allowing for future myelination. Restoration of neural architecture appeared to initiate earlier in the end-to-end repair group, as reflected by gradual reorganization of the nerve and formation of perineurium. Electron microscopy images and a detailed description of findings appear in Figure 5 and the accompanying caption.

Discussion

Although rodent models are used widely in the study of peripheral nerve regeneration, the selection of experimental time points for histological assessment is often based on limited data. In this study, we sought to provide benchmarks for regeneration at various time points by recording histomorphometric parameters over 24 months. An unexpected finding was that little fluctuation in fiber counts occurred beyond 3 months. This observation was further corroborated by quantitative assessment of motor neuron pools by retrograde labeling of motor neuron cell bodies in the ventral horn. Prior work in a transection and repair model had found a peak in fiber count and density at 3 months, as in this study, but with a modest decrease in measures between 6 and 24 months.[13] This pattern of decline was not evident in this study.

Although nerve fiber counts reached a plateau within 3 months for both experimental groups, the point at which fiber counts leveled off differed significantly. After end-to-end repair, the fiber counts were almost 50% greater than those achieved with nerve grafting. This difference persisted over the subsequent 18 months that animals were followed. Thus, there appeared to be either a decrement in regenerating fibers across the second suture line or along the course of the graft that was lasting. This observation is consistent with early work on nerve regeneration that reported decrease in fiber counts distal to repairs[17,18] and may have clinical relevance, as grafts are often used to minimize tension across a suture line.[19,20] While severe degrees of tension may predispose to scarring and ischemia in a regenerating nerve, modest levels of tension across nerve repairs are well tolerated and do not significantly impair regeneration.[21] A recent study in sciatic nerve found that a six suture repair resulted in greater collagen deposition than three sutures.[22] Also noted was an increase in nerve fiber counts within the isograft when compared to distal counts. The elevated number within the graft can be attributed to increased collateral sprouting within

the graft.[23–25] Interestingly, the mid-graft fiber counts are similar in magnitude to the fiber counts of the cut and repair group. This observation provides further support for the premise that a portion of regenerating nerve fibers fail to successfully navigate across sutured repairs.[17,18]

We also observed that not all histomorphometric parameters change over the same time course. Whereas fiber counts and measurements of nerve density stabilized at 3 months, measures of fiber maturity, such as myelination and percent neural tissue, continued to show a trend of increase over the course of 12 months. No significant changes in nerve characteristics were observed between 12 and 24 months. The motor neuron count of the end-to-end repair was consistent over the time course of evaluation (1 and 3 months). In contrast, the motor neuron pool of the graft group expanded significantly from 1 to 3 months. The change in motor neuron pool size of the graft group reflect significant ongoing regeneration over the monitored time frame, while the lack of significant increase in the cut repair indicates that most motor axons successfully reached the distal stump by 1 month. The increase in the graft group over the same time course illustrates the difference in regenerative challenge posed to regenerating axons by the addition of increased regeneration length (1 cm graft) and an additional distal suture line. The combined effect is increased regeneration time and fewer regenerating motor neurons compared to end-to-end repair. Our data also indicated that retrograde labeling allows for detection of regenerating motor neurons that have not yet become myelinated and are thus not detectable on light microscopy. The motor neuron labeling in the nerve graft group despite negative light histology prompted use of electron microscopy to confirmed presence of unmyelinated fibers. Unmyelinated fibers can be quantified using electron microscopy and other techniques such as immunohistochemical staining. The use of motor neuron labeling also allowed for assessment of motor neuron specific regeneration (harvest of dorsal root ganglia may be used to assess sensory neuron regeneration).

The clearance of fiber debris occurred over 9 months and reflects the gradual replacement of degenerated tissue. The clearance of myelin debris in the graft group was delayed in comparison to the transection repair. The percent fiber debris, an indirect measure of WD, of the graft group peaked at 3 months and returned to baseline by 6 months. In contrast, the percent fiber debris of the end-to-end repair was at baseline levels by month 3. During WD, axons recede 1–2 mm from the site of injury, and myelin debris is phagocytosed by macrophages. The removal of debris is essential for subsequent axonal regeneration and delays in WD can delay recovery.[26–28] While the cause of the delay in WD of the graft group is unknown, several factors likely contribute. The interposition of the graft between the proximal and distal nerve stumps provides additional axonal tissue that must be cleared during WD. The additional load of neural myelin debris associated with a sizable interpositional nerve graft may contribute to the delay in WD. Another contributing factor is the migration time of nonresident macrophages that are the major cell mediators of WD. The lack of continuity in vasculature of the graft may limit macrophage infiltration into the graft and thus slow WD.

Whereas, we had anticipated an initial rise in fiber counts from an abundance of sprouts followed by a substantial drop in fiber counts, this pattern was not observed. Transected

peripheral nerves typically regenerate with multiple axon sprouts arising from each nerve fiber.[23–25] It is possible that this initial burst of regeneration (and the subsequent decline) was not captured during the time points studied. Another possibility is that the process of sprouting and pruning is more dynamic than previously recognized, with some nerves sprouting as others are pruned. In analyzing our data, we limited our outcome measures to binary image analysis (quantitative histomorphometry) and retrograde labeling. While these methods provide a detailed picture of nerve regeneration, we acknowledge that other approaches are also effective. Future work may be particularly helpful in further defining how differences in histological techniques relate to functional outcomes.

Pruning behavior after nerve injury occurs in both motor and sensory peripheral nerve fibers. Motor neurons within mixed nerves will preferentially reinnervate motor targets, a process mediated by pruning collaterals from cutaneous pathways. This phenomenon has been termed preferential motor reinnvervation.[29] Similarly, although sensory nerve will regenerate equally down a sensory nerve graft without distal target and a sensory nerve with intact distal receptors, fibers directed down the nerve graft are eventually pruned whereas the fibers that reach distal receptors are preserved.[30,31] These observations are analogous to the stereotypical pruning observed in neural development. Advances in the study of axonal guidance have begun to elucidate the molecular mechanisms that mediate axonal path-finding.[32] In particular, the ephrin-B proteins have been studied for their role in influencing axon pathfinding by repulsion.[33] The phenomenon of pruning is well described both in development[34] and disease.[35] Advances in nerve imaging coupled with increasing availability of transgenic mice that express spectral variants of fluorescent chromophores[36–38] may provide further insights into these phenomena.

Data on the natural history of regeneration after nerve reconstruction provides a valuable benchmark for future studies on nerve regeneration. We observed that the differences in fiber count after end-to-end repair versus a nerve graft repair persisted for the full 2-year duration of the study. Over a shorter time course, another study demonstrated that at 6 months regenerating axon fibers are still maturing.[39] Our findings are significant because in some small animal experiments only a narrow window of opportunity exists for detecting differences between experimental groups.[14] The animals' inherent capacity for nerve regeneration and small limb length are thought to explain this finding. For example, in the mouse model, an early 3-week endpoint is optimal for study of the nerve allograft response and histomorphometry.[40] The persisting differences in fiber count between the graft and end-to-end repair are consistent with our previous findings on timing. The timing of evaluation becomes crucial during experimental comparisons of therapeutic interventions for the same nerve injury (i.e., isograft vs. conduit[41] or isograft vs. nonimmunosuppressed fresh allograft[14]). Our current results reinforce previous findings[42] that different levels of nerve injury (e.g., crush, transection/repair, and transection/grafting) result in graded levels of functional recovery. Further, this study reaffirms the legitimacy of the small animal model in study of regeneration, and new approaches to accelerate nerve regeneration hold promise for improving functional recovery through early reinnervation.

Conclusion

Peripheral nerve regeneration after nerve transection injury differs from regeneration after nerve gap injury in a rodent model. End-to-end repair of a transection injury resulted in significantly higher fiber counts and motor neuron counts compared with nerve grafting of a nerve gap injury for all time points up to 2 years. Both types of injury result in an early plateau in fiber count and motor neuron counts at 3 months, implying a limited overall impact of pruning on morphometric parameters. These data provide a detailed depiction of nerve regeneration after nerve injury and afford insights into the decrement of nerve regeneration that may occur across graft repairs.

Acknowledgments

Grant sponsor: National Institutes of Health; Grant number: 2R01 NS33406-12; Grant sponsor: National Institutes of Health; Grant number T32 DC 0022-15

References

1. Nguyen QT, Sanes JR, Lichtman JW. Pre-existing pathways promote precise projection patterns. Nat Neurosci. 2002; 5:861–867. [PubMed: 12172551]
2. Jensen JN, Brenner MJ, Tung TH, Hunter DA, Mackinnon SE. Effect of FK506 on peripheral nerve regeneration through long grafts in inbred swine. Ann Plast Surg. 2005; 54:420–427. [PubMed: 15785285]
3. Myckatyn TM, MacKinnon SE. A review of research endeavors to optimize peripheral nerve reconstruction. Neurol Res. 2004; 26:124–138. [PubMed: 15072631]
4. Kokai LE, Bourbeau D, Weber D, McAtee J, Marra KG. Sustained growth factor delivery promotes axonal regeneration in long gap peripheral nerve repair. Tissue Eng Part A. 2011; 17:1263–1275. [PubMed: 21189072]
5. Harvey PA, Lee DH, Qian F, Weinreb PH, Frank E. Blockade of Nogo receptor ligands promotes functional regeneration of sensory axons after dorsal root crush. J Neurosci. 2009; 29:6285–6295. [PubMed: 19439606]
6. Ao Q, Fung CK, Tsui AY, Cai S, Zuo HC, Chan YS, Shum DK. The regeneration of transected sciatic nerves of adult rats using chitosan nerve conduits seeded with bone marrow stromal cell-derived Schwann cells. Biomaterials. 2011; 32:787–796. [PubMed: 20950852]
7. Erba P, Mantovani C, Kalbermatten DF, Pierer G, Terenghi G, Kingham PJ. Regeneration potential and survival of transplanted undifferentiated adipose tissue-derived stem cells in peripheral nerve conduits. J Plast Reconstr Aesthet Surg. 2010; 63:e811–817. [PubMed: 20851070]
8. Haastert-Talini K, Schmitte R, Korte N, Klode D, Ratzka A, Grothe C. Electrical stimulation accelerates axonal and functional peripheral nerve regeneration across long gaps. J Neurotrauma. 2011; 28:661–674. [PubMed: 21265597]
9. Hamilton SK, Hinkle ML, Nicolini J, Rambo LN, Rexwinkle AM, Rose SJ, Sabatier MJ, Backus D, English AW. Misdirection of regenerating axons and functional recovery following sciatic nerve injury in rats. J Comp Neurol. 2011; 519:21–33. [PubMed: 21120925]
10. Huang J, Lu L, Hu X, Ye Z, Peng Y, Yan X, Geng D, Luo Z. Electrical stimulation accelerates motor functional recovery in the rat model of 15-mm sciatic nerve gap bridged by scaffolds with longitudinally oriented microchannels. Neurorehabil Neural Repair. 2010; 24:736–745. [PubMed: 20702391]
11. Wan LD, Xia R, Ding WL. Electrical stimulation enhanced remyelination of injured sciatic nerves by increasing neurotrophins. Neuroscience. 2010; 169:1029–1038. [PubMed: 20553821]
12. Yeh CC, Lin YC, Tsai FJ, Huang CY, Yao CH, Chen YS. Timing of applying electrical stimulation is an important factor deciding the success rate and maturity of regenerating rat sciatic nerves. Neurorehabil Neural Repair. 2010; 24:730–735. [PubMed: 20705804]

13. Mackinnon SE, Dellon AL, O'Brien JP. Changes in nerve fiber numbers distal to a nerve repair in the rat sciatic nerve model. Muscle Nerve. 1991; 14:1116–1122. [PubMed: 1745287]
14. Brenner MJ, Moradzadeh A, Myckatyn TM, Tung TH, Mendez AB, Hunter DA, Mackinnon SE. Role of timing in assessment of nerve regeneration. Microsurgery. 2008; 28:265–272. [PubMed: 18381659]
15. Sangster CL, Galea MP, Fan R, Morrison WA, Messina A. A method for processing fluorescent labelled tissue into methacrylate: A qualitative comparison of four tracers. J Neurosci Methods. 1999; 89:159–165. [PubMed: 10491947]
16. Hunter DA, Moradzadeh A, Whitlock EL, Brenner MJ, Myckatyn TM, Wei CH, Tung TH, Mackinnon SE. Binary imaging analysis for comprehensive quantitative histomorphometry of peripheral nerve. J Neurosci Methods. 2007; 166:116–124. [PubMed: 17675163]
17. Almquist EE, Smith OA, Fry L. Nerve conduction velocity, microscopic, and electron microscopy studies comparing repaired adult and baby monkey median nerves. J Hand Surg Am. 1983; 8:406–410. [PubMed: 6886334]
18. Chor HCH, Davenport RE, Dolkhart RE, Beard G. Atrophy and regeneration of the gastrocnemius-soleus muscles. JAMA. 1939; 113:1029–1033.
19. Gu X, Ding F, Yang Y, Liu J. Construction of tissue engineered nerve grafts and their application in peripheral nerve regeneration. Prog Neurobiol. 2011; 93:204–230. [PubMed: 21130136]
20. Siemionow M, Bozkurt M, Zor F. Regeneration and repair of peripheral nerves with different biomaterials: review. Microsurgery. 2010; 30:574–588. [PubMed: 20878689]
21. Sunderland IR, Brenner MJ, Singham J, Rickman SR, Hunter DA, Mackinnon SE. Effect of tension on nerve regeneration in rat sciatic nerve transection model. Ann Plast Surg. 2004; 53:382–387. [PubMed: 15385776]
22. Martins RS, Teodoro WR, Simplicio H, Capellozi VL, Siqueira MG, Yoshinari NH, Pereira JP, Teixeira MJ. Influence of suture on peripheral nerve regeneration and collagen production at the site of neurorrhaphy: An experimental study. Neurosurgery. 2011; 68:765–772. [PubMed: 21164381]
23. Jenq CB, Coggeshall RE. Effects of sciatic nerve regeneration on axonal populations in tributary nerves. Brain Res. 1984; 295:91–100. [PubMed: 6713180]
24. Jenq CB, Coggeshall RE. Numbers of regenerating axons in parent and tributary peripheral nerves in the rat. Brain Res. 1985; 326:27–40. [PubMed: 3971147]
25. Morris JH, Hudson AR, Weddell G. A study of degeneration and regeneration in the divided rat sciatic nerve based on electron microscopy. II. The development of the “regenerating unit”. Z Zellforsch Mikrosk Anat. 1972; 124:103–130. [PubMed: 5011137]
26. Brown MC, Lunn ER, Perry VH. Consequences of slow Wallerian degeneration for regenerating motor and sensory axons. J Neurobiol. 1992; 23:521–536. [PubMed: 1431835]
27. Boivin A, Pineau I, Barrette B, Filali M, Vallieres N, Rivest S, Lacroix S. Toll-like receptor signaling is critical for Wallerian degeneration and functional recovery after peripheral nerve injury. J Neurosci. 2007; 27:12565–12576. [PubMed: 18003835]
28. Genden EM, Watanabe O, Mackinnon SE, Hunter DA, Strasberg SR. Peripheral nerve regeneration in the apolipoprotein-E-deficient mouse. J Reconstr Microsurg. 2002; 18:495–502. [PubMed: 12177820]
29. Brushart TM, Gerber J, Kessens P, Chen YG, Royall RM. Contributions of pathway and neuron to preferential motor reinnervation. J Neurosci. 1998; 18:8674–8681. [PubMed: 9786974]
30. Mackinnon SE, Dellon AL, Hudson AR, Hunter DA. Chronic human nerve compression-a histological assessment. Neuropathol Appl Neurobiol. 1986; 12:547–565. [PubMed: 3561691]
31. Mackinnon SE, Dellon AL, Lundborg G, Hudson AR, Hunter DA. A study of neurotrophism in a primate model. J Hand Surg Am. 1986; 11:888–894. [PubMed: 3794250]
32. Patel BN, Van Vactor DL. Axon guidance: The cytoplasmic tail. Curr Opin Cell Biol. 2002; 14:221–229. [PubMed: 11891122]
33. Xu NJ, Henkemeyer M. Ephrin-B3 reverse signaling through Grb4 and cytoskeletal regulators mediates axon pruning. Nat Neurosci. 2009; 12:268–276. [PubMed: 19182796]

34. Low LK, Cheng HJ. Axon pruning: An essential step underlying the developmental plasticity of neuronal connections. Philos Trans R Soc Lond B Biol Sci. 2006; 361:1531–1544. [PubMed: 16939973]
35. Luo L, O'Leary DD. Axon retraction and degeneration in development and disease. Annu Rev Neurosci. 2005; 28:127–156. [PubMed: 16022592]
36. Magill C, Whitlock E, Solowski N, Myckatyn T. Transgenic models of nerve repair and nerve regeneration. Neurol Res. 2008; 30:1023–1029. [PubMed: 19079976]
37. Magill CK, Moore AM, Borschel GH, Mackinnon SE. A new model for facial nerve research: The novel transgenic Thy1-GFP rat. Arch Facial Plast Surg. 2010; 12:315–320. [PubMed: 20855773]
38. Myckatyn TM, Mackinnon SE, Hunter DA, Brakefield D, Parsadanian A. A novel model for the study of peripheral-nerve regeneration following common nerve injury paradigms. J Reconstr Microsurg. 2004; 20:533–544. [PubMed: 15534781]
39. Muratori L, Ronchi G, Raimondo S, Giacobini-Robecchi MG, Fornaro M, Geuna S. Can regenerated nerve fibers return to normal size? A long-term post-traumatic study of the rat median nerve crush injury model. Microsurgery. 201210.1002/micr.21969
40. Ray WZ, Kasukurthi R, Kale SS, Santosa KB, Hunter DA, Johnson P, Yan Y, Mohanakumar T, Mackinnon SE, Tung TH. Costimulation blockade inhibits the indirect pathway of allorecognition in nerve allograft rejection. Muscle Nerve. 2011; 43:120–126. [PubMed: 21171102]
41. Whitlock EL, Tuffaha SH, Luciano JP, Yan Y, Hunter DA, Magill CK, Moore AM, Tong AY, Mackinnon SE, Borschel GH. Processed allografts and type I collagen conduits for repair of peripheral nerve gaps. Muscle Nerve. 2009; 39:787–799. [PubMed: 19291791]
42. Hare GM, Evans PJ, Mackinnon SE, Best TJ, Bain JR, Szalai JP, Hunter DA. Walking track analysis: A long-term assessment of peripheral nerve recovery. Plast Reconstr Surg. 1992; 89:251–258. [PubMed: 1732892]

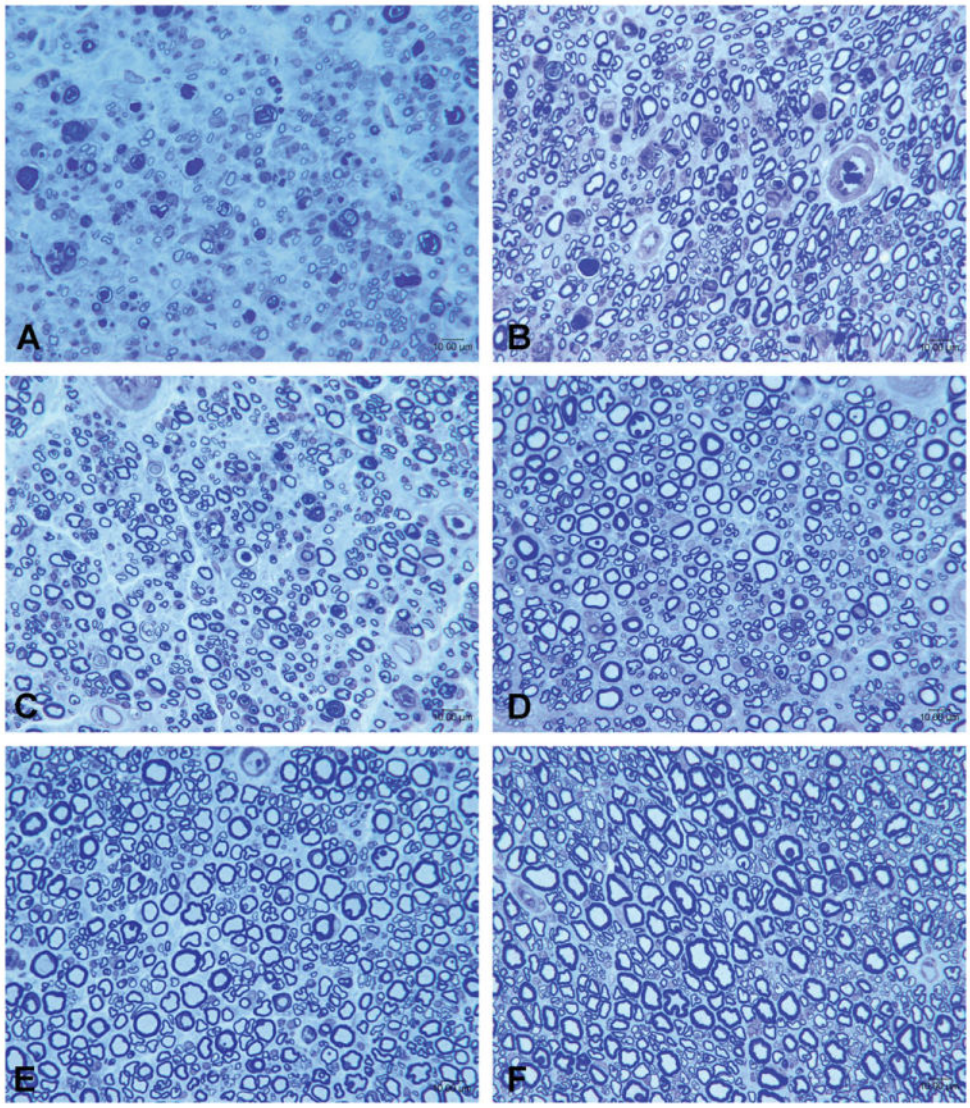

Figure 1.

Representative photomicrographs of sciatic nerves after end-to-end repair groups in animals sacrificed at serial time points. **A:** 1 month; **B:** 3 months; **C:** 6 months; **D:** 9 months; **E:** 12 months; **F:** 24 months. [Color figure can be viewed in the online issue, which is available at wileyonlinelibrary.com.]

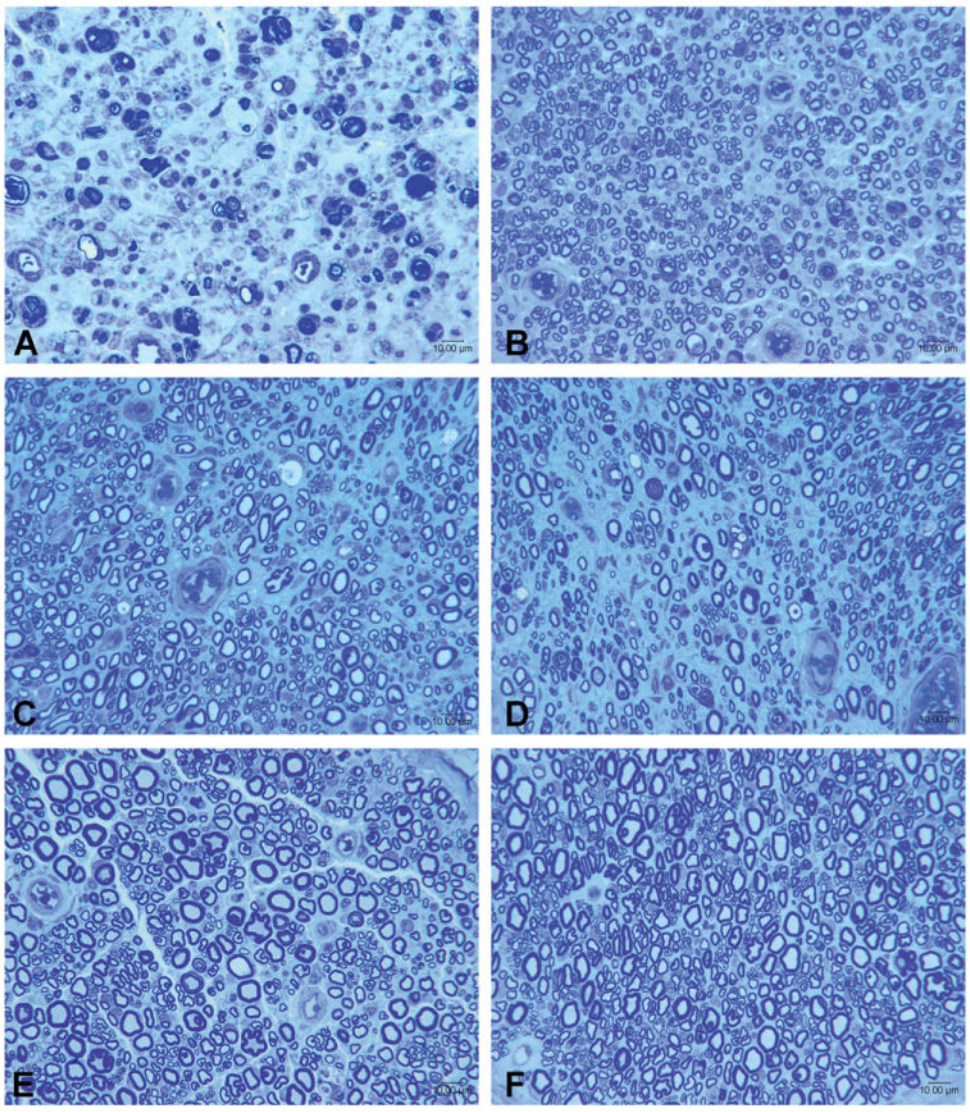

Figure 2.

Representative photomicrographs of sciatic nerves from animals undergoing nerve grafting sacrificed at serial time points, with sections taken distal to isograft. **A:** 1 month; **B:** 3 months; **C:** 6 months; **D:** 9 months; **E:** 12 months; **F:** 24 months. [Color figure can be viewed in the online issue, which is available at wileyonlinelibrary.com.]

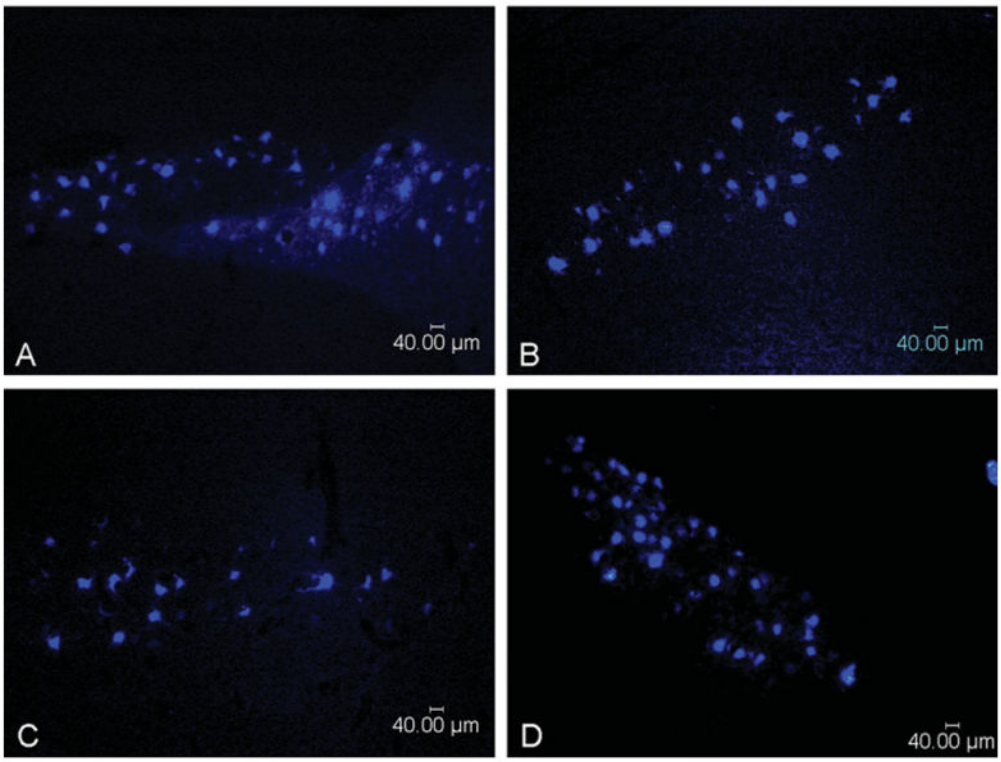

Figure 3.

Representative photomicrographs of retrograde labeled motor neuron cell bodies from spinal cord ventral horn. **A:** End-to-end repair at 3 months. **B:** End-to-end repair at 24 months. **C:** Nerve graft repair at 1 month. **D:** Nerve graft repair at 24 months. [Color figure can be viewed in the online issue, which is available at wileyonlinelibrary.com.]

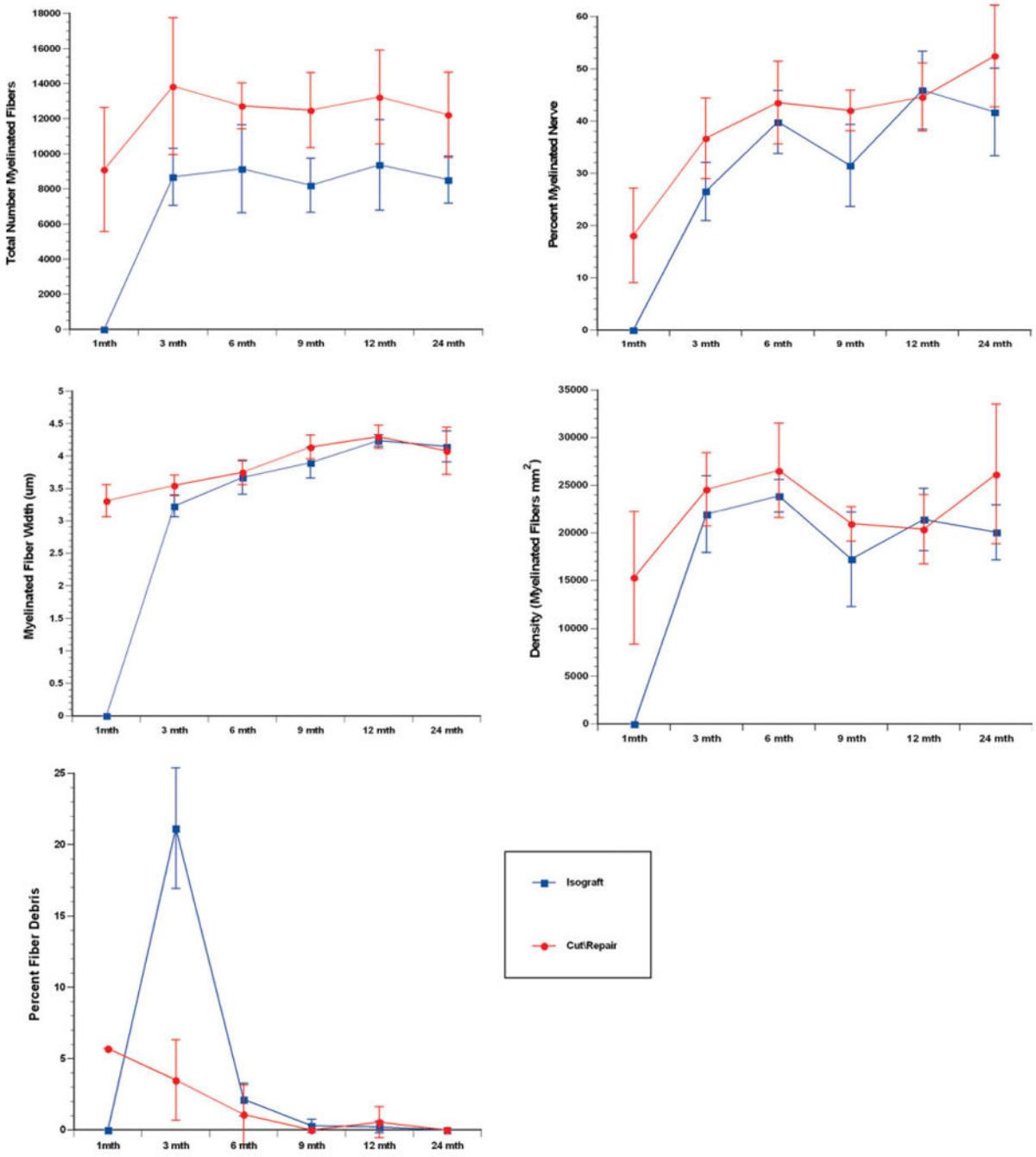

Figure 4.

Histomorphometric comparison of end-to-end repair versus nerve graft repair groups at serial time points. Parameters of nerve density, fiber count, percent neural tissue, myelin width, and percent neural debris are shown. Fiber counts and nerve density demonstrated plateau at 3 months, whereas myelin width and percent neural tissue increased through 12 months. Clearance of myelin debris occurred over the initial 9 months after original injury. [Color figure can be viewed in the online issue, which is available at wileyonlinelibrary.com.]

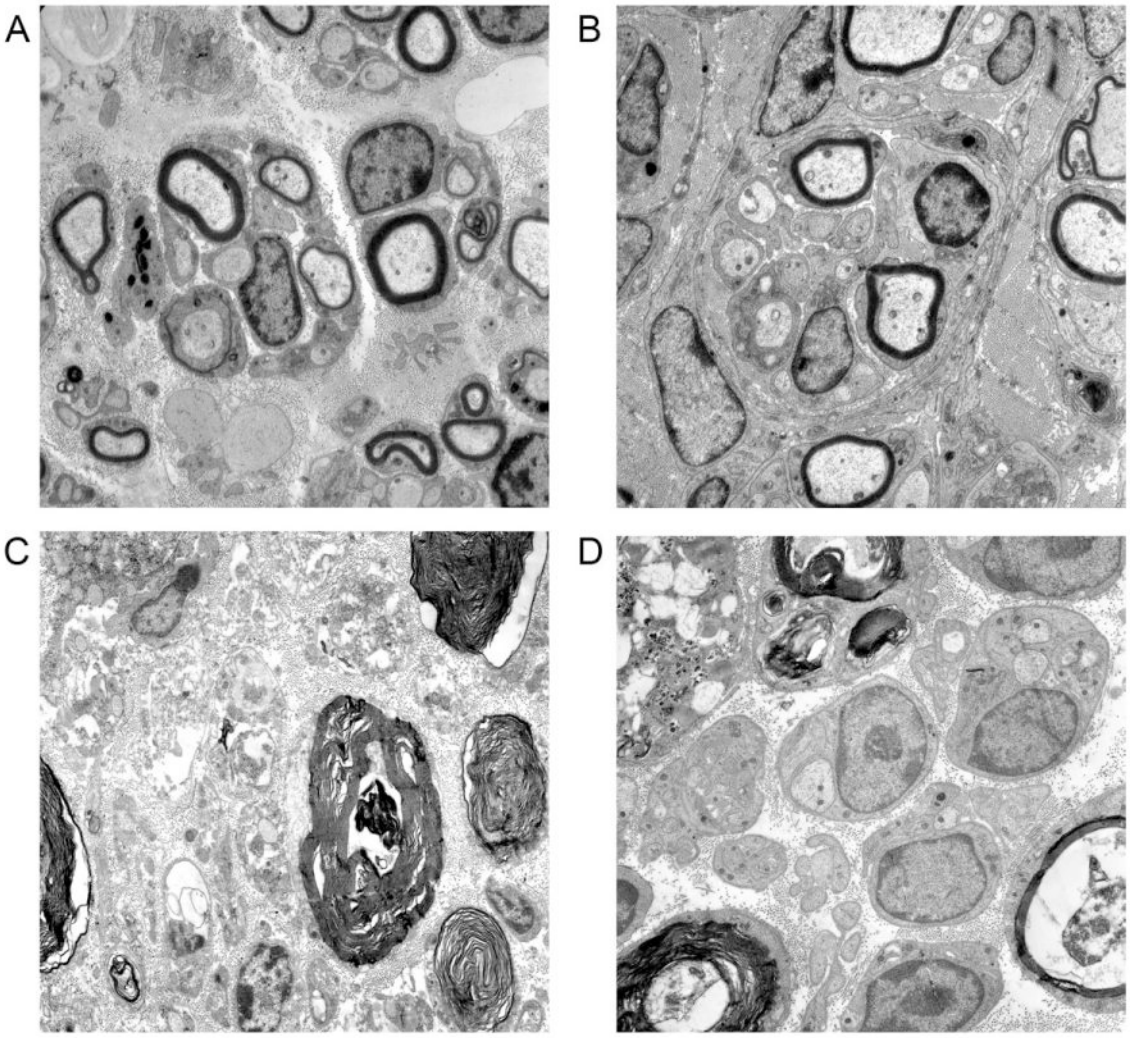

Figure 5.

Electron microscopy of nerves at 1 month after end-to-end repair versus nerve grafting (4600x). **A:** Distal nerve section after end-to-end repair at 1 month shows a combination of myelinated and unmyelinated fibers. Two regenerating units are present in the center of the figure, with early myelination around several fibers. Schwann cells have speckled nuclei, with basal lamina visible at the periphery of the unit on right. **B:** Another distal section of the same repaired nerve demonstrates a large regenerating unit in the center, with myelinated and unmyelinated fibers. **C:** In the nerve graft group, WD is still evident in this section distal of the graft. In the middle of the figure is a degenerating nerve fiber. More advanced stages of WD are shown in the lower right, with a thumbprint type appearance. **D:** Another section distal to the nerve graft shows Schwann cell nuclei with classic double basal laminae associated with immature, but yet unmyelinated, nerve fibers. A lipid-laden macrophage (upper left) has phagocytosed debris, allowing for clearance of myelin and reorganization of regenerating nerve.